Electronic Transport between Graphene Layers Covalently Connected by Carbon Nanotubes

Frederico D. Novaes,[†] Riccardo Rurali,[†] and Pablo Ordejón[‡],*

[†]Institut de Ciència de Materials de Barcelona (CSIC), Campus UAB, 08193 Bellaterra, Barcelona, Spain, and [‡]Centre d'Investigació en Nanociència i Nanotecnologia—CIN2 (CSIC-ICN), Campus UAB, 08193 Bellaterra, Spain

ABSTRACT We present a first-principles study of the electronic transport properties of metallic and semiconducting carbon nanotube (CNT) junctions connecting two graphene layers, for different CNT lengths and link structures. Transport is analyzed in terms of the scattering states originated from the π and π^* states of the finite-length CNTs, which couple to the graphene states producing resonances in the transmission curves. We find that, for metallic CNTs, the conductance is nearly independent of the tube length, but changes strongly with the link structure, while the opposite occurs for semiconducting CNTs, where the conductance in the tunneling regime is mainly controlled by the tube length and independent of the link structure. The sizable band offset between graphene and the CNTs yields to considerable effects on the transport properties, which cannot be captured using simple empirical models and highlights the need for a first-principles description.

The study of electronic transport both in carbon nanotubes and in graphene has been the focus of a great deal of work[1,2] owing to the intriguing fundamental phenomena that these materials exhibit, and the promise of outstanding applications in nanoelectronics. Despite having the same chemical composition and local atomic structure (sp^2 carbon), the electronic properties of these nanostructures depend dramatically on their topology and intermediate and long-range structure (*e.g.*, chirality for nanotubes, edges for graphene). This variety of properties allows for a plethora of different applications, in many of which the formation of junctions between parts with distinct electronic properties plays an essential role.

Here, we consider the possibility of future devices that may use combinations of graphene layers and CNTs for nanoelectronics applications. For instance, nanotubes might be used as interconnects to transmit signals between two graphene-based nanodevices, in the same way as metallic wires do between traditional silicon-based transistors. One might also envision more ambitious scenarios,[3] in which nanotubes could be used as vertical connections in three-dimensional architectures that would provide a better use of chip space. In these 3D circuits, nanotube transistors could be used as switches to reconfigure the circuit's function. In any of these or other possible applications, understanding the transport properties of graphene–nanotube connections is a prerequisite, and the objective of this paper.

We present first-principles studies of the geometry, electronic structure, and transport properties of systems consisting on single-walled carbon nanotubes connecting two graphene sheets. We consider CNTs with different chiralities (both metallic and semiconducting) and lengths, and compute the conductance between the two sheets through the nanotube. In the structures studied here, graphene and nanotubes are linked covalently in a seamless sp^2 structure. Such connections are expected to provide the best conductance characteristics, since they are the weakest perturbing links and preserve the chemistry and local sp^2 bonding of both nanotubes and graphene, in contrast with links achieved by chemical functionalization (*e.g., via* peptide and disulfide links) considered by other authors.[4]

Experimental evidence for the possibility of building such a connection has been provided by some recent works. Kondo *et al.*[5] reported the synthesis, by means of chemical vapor deposition techniques, of composite structures with horizontal graphene multilayers connected to vertically aligned multiwalled carbon nanotubes. Refinement of this technique could possibly yield methods to build graphene–nanotube contacts in a controlled manner. More recently, Kane *et al.*[6] have suggested that highly conductive con-

*Address correspondence to pablo.ordejon@cin2.es.

tacts between platinum electrodes and nanotubes, obtained by a high temperature annealing treatment, are due to the formation of a graphene layer on the metallic surface, which is thought to be covalently linked to the nanotube. These works seem to indicate that, besides their experimental feasibility, such connections should have good conductance characteristics.

From the theoretical side, graphene−CNT covalent interconnections have been previously considered in the literature, although these works did not focus on the electronic transport properties. Matsumoto and Saito[7] were the first to study such structures, focusing on the geometry and electronic states of graphene sheets with a periodic arrangement of covalently linked (6,6) CNTs in a triangular lattice, using an sp^3 nonorthogonal tight-binding (TB) model, and local density approximation (LDA) calculations only for selected systems. More recently, González et al.[8] have presented a detailed study of the electronic properties of links between graphene and metallic armchair $(6n, 6n)$ and zigzag $(6n,0)$ CNTs, using a simple π orbital TB Hamiltonian and a continuum theory based on Dirac fermion fields. They considered the case of junctions of a single nanotube with a single infinite graphene layer, as well as periodic arrays of junctions in a triangular lattice like those studied by Matsumoto and Saito. In both studies, the geometry of the junctions has six heptagons evenly spaced along the link between graphene and CNT, and no edges or termination of the graphene layer(s) were considered. The systems are therefore highly symmetric, maintaining the C_{6v} symmetry of graphene. Finally, Dimitrakakis et al.[9] and Varshney et al.[10] also considered 3D structures of graphene layers linked by nanotubes, but they focused on the possible hydrogen storage applications and on their thermal transport properties, rather than the electronic transport. This is, therefore, the first study of the electronic transport between graphene sheets through covalently linked nanotube junctions.

RESULTS AND DISCUSSION

Our goal of studying both semiconducting and metallic CNTs implies that we must consider chiralities (n,m) different from the $(6n,6n)$ and $(6n,0)$ investigated in previous studies,[7,8] which are all metallic (as occurs for nanotubes with $(n − m) = 3l$, with l being zero or any positive integer[11,12]). In general, covalent links between any (n,m) CNT and graphene can be accomplished, but the resulting structures have a symmetry lower than C_{6v} with a more irregular arrangement of heptagons, and possibly showing the presence of rings other than hexagons and heptagons. Baowan et al.[13] have considered the possible ways in which armchair (4,4) and zigzag (8,0) nanotubes can be attached covalently to graphene to form a seamless sp^2 structure, finding a large number of possibilities with different numbers and sizes of rings (from tetragonal to decago-
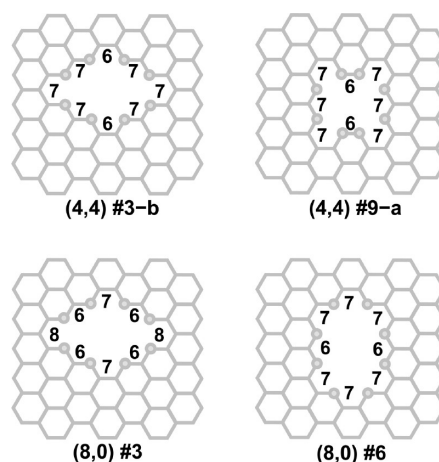

Figure 1. Scheme of the connection of graphene with the (4,4) and (8,0) CNTs for the different structures considered. The small circles show the carbon atoms from graphene that bind to the atoms of the nanotube edge (not shown). The numbers indicate the sizes of the rings that result at each site upon the nanotube attachment.

nal). Here, we have considered some of the structures proposed by Baowan et al., for the metallic armchair (4,4) and the semiconducting zigzag (8,0) CNTs, both having similar diameter (making the comparison of the transport properties more relevant). From all the possible structures of the link with graphene, we have selected only two for each nanotube that, *a priori*, seem more reasonable, shown in Figure 1. For the (4,4) tube, we consider the two link structures that have only six heptagonal defect rings in the junction between graphene and the nanotube (denoted as #3-b and #9-a by Baowan et al.). For the (8,0) tube, we also consider two structures: the only one that has only six heptagonal rings and one that has two heptagonal and two octagonal rings (denoted as #6 and #3, respectively, by Baowan et al.). All these structures present a C_{2v} symmetry, which is a reduced one in comparison with the symmetries of the graphene sheet and the nanotubes.

For the relaxed structures (see Methods), we calculate the conductance from first-principles, by means of the TranSiesta method,[14] within the nonequilibrium Green's function (NEGF) formalism. The system is divided into left and a right leads and a central scattering region.[15] The problem is solved in the scattering region, using the open boundary conditions imposed by the leads (in our case, semi-infinite graphene layers) through their self-energies. The central region includes the CNT and the portion of graphene layers around the junction with their hydrogen termination (see Figure 2). For computational convenience, as it is frequently done in this kind of calculations, we consider periodic boundary conditions in the direction perpendicular to the transport (x axis in Figure 2). Therefore, we are actually computing the conductance through a periodic linear array of nanotubes connecting two semi-infinite
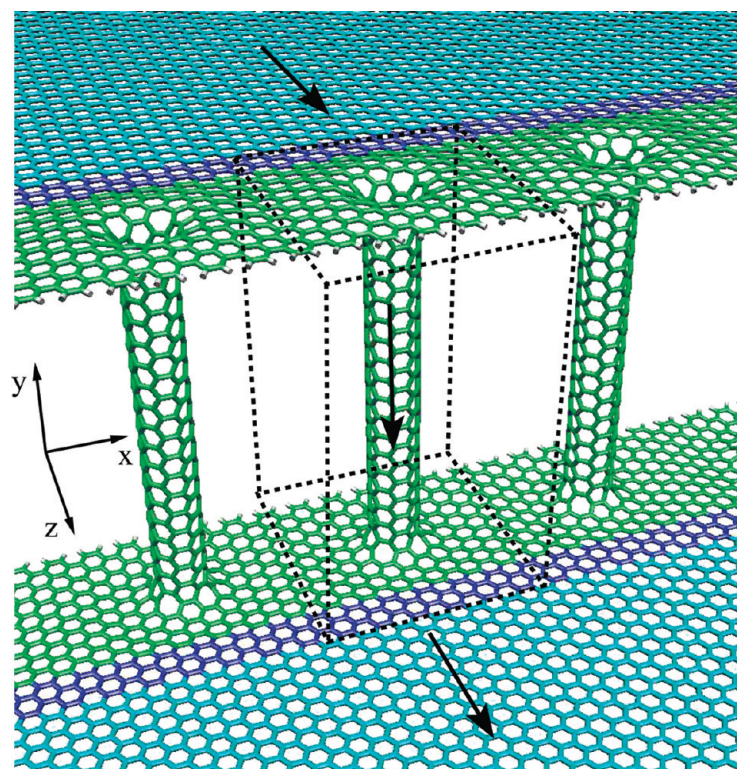
Figure 2. Setup used for the transport calculations: an array of nanotubes connecting two semi-infinite graphene sheets. The dotted lines enclose the atoms explicitly considered in the simulation box, which is repeated periodically in the *x* direction. The scattering region (shown in green) includes the CNT, the graphene−CNT junctions and part of the graphene sheet (including the H-saturated edges). The leads (in blue) are ideal, semi-infinite two-dimensional graphene sheets, where the darker areas correspond to the atoms explicitly considered in the simulation box in the calculation of the NEGF's, while lighter areas are described through self-energies.

graphene sheets, and careful *k*-point sampling in this direction (*i.e.*, along the graphene edge and the nanotube array) is required to obtain reliable results for the conductance.[16] We denote the *k*-points along the edge direction as $k_\parallel$. The conductance calculated in this manner is that of a single repeated cell (*i.e.*, the conductance through each of the CNTs contacting the graphene sheets). The implications of our calculations for the limit of a single CNT connection will be discussed in detail below.
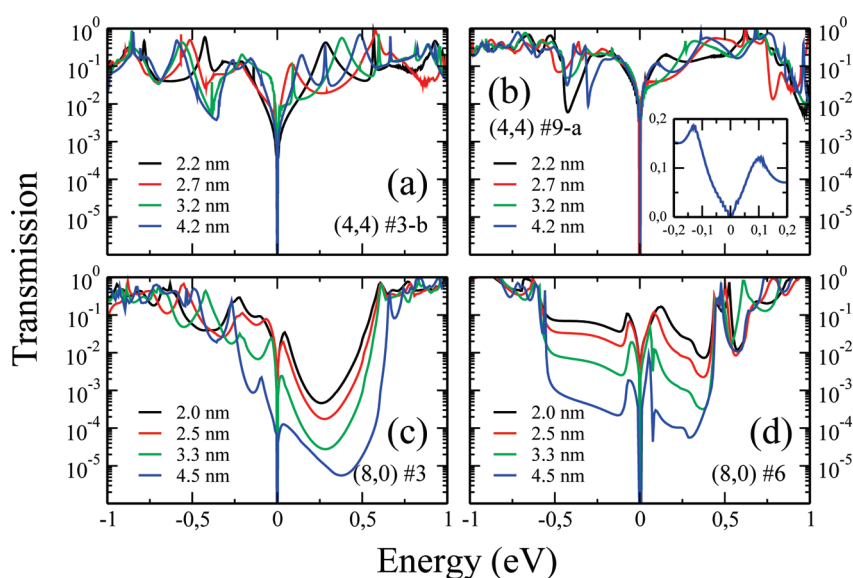
Figure 3. Transmission (shown in logarithmic scale) *versus* energy (referred to the Fermi level) of the graphene−nanotube junctions: (a) (4,4), link #3-b; (b) (4,4), link #9-a; (c) (8,0), link #3; (d) (8,0), link #6. For each junction, different curves correspond to different nanotube lengths, as indicated in the legend. The inset in panel b shows a linear scale plot of the transmission around the Fermi energy for the 4.2 nm (4,4) nanotube with link #9-a.
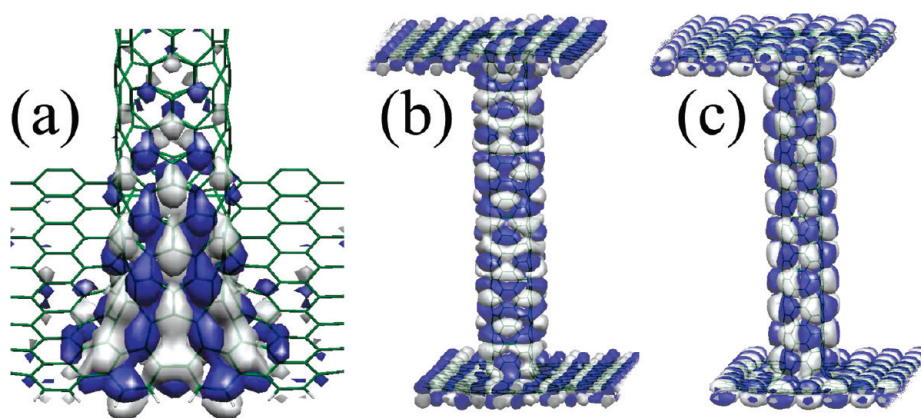
Figure 4. (a) Contour plot of a quasi-localized wave function confined at the interface between graphene and the (8,0) nanotube, for the #6 link. The state corresponds to the transmission peak located just above the Fermi energy in Figure 3d. Graphics b and c show the two scattering states for the (4,4) nanotube #9-a link, at $E = 0.36$ eV, corresponding to the two transmission eigenchannels shown with full and dashed lines in Figure 6a, respectively.

Figure 3 is a summary of our transport calculations, showing the transmission curves for four different nanotube lengths (from around $2-5$ nm) for each of the four types of junctions.

For metallic (4,4) tubes, the transmission has values in the range from 0.01 to 1, in the energy window considered. The drop in the conductance at the Fermi level is due to the semimetallic character of graphene, and will be discussed later. Oscillations are present owing to the discrete structure of electronic states in the nanotube, which depends on its particular length. This leads to a different structure of peaks for each length, which becomes denser for longer nanotubes, as expected. The structure of the link also has a strong effect on the transmission curves, which are considerably different due to the different coupling between graphene and CNT states for each link structure. For the range of lengths considered here, the average transmission is essentially independent of the length of the CNT, a clear indication of ballistic transport through strongly propagating and delocalized nanotube states. Our results for metallic nanotubes give support to the recent suggestion of improved contact characteristics of nanotubes on platinum electrodes upon formation of a graphene layer on the metallic surface.[6]

For semiconducting (8,0) tubes, a wide low-transmission region around the Fermi level is clearly observed, corresponding to the forbidden energy gap of the pristine, infinite nanotube (0.8 eV). The transmission outside this gap is relatively large and close to unity, as for metallic nanotubes, which indicates ballistic conduction at energies at which the nanotube sustains valence or conduction states. Therefore, doped nanotubes (for which the Fermi level is located within the band edges) should be expected to have transport properties similar to those of metallic nanotubes. Within the gap, the transmission is considerably smaller, but far from negligible, specially for the shorter nanotubes. This is due to the existence of metal-induced gap states (MIGS) within the gap of the nanotube, which de-

cay exponentially from the graphene−nanotube interface. This yields an exponential dependence of the transmission with nanotube length, characteristic of the tunneling regime. Again, the structure of the link strongly affects the shape and values of the transmission curves. Part of this difference is associated with the fact that the location of the band gap of the nanotube with respect to the Fermi level of graphene differs for both links, implying a different band alignment for each structure. This can be traced back to the different strains of the (8,0) nanotube for the two types of connections: the #3 link produces a strong distortion of the nanotube, from the ideal circular section to a pronouncedly flat one. This strain produces an upward shift of the CNT bands which leads to a different band alignment with the graphene sheet. Therefore, engineering the contact structure could be used to tune somewhat the transport properties of the CNT−graphene links.

In the transmission curves for the (8,0) nanotube, we observe the appearance of some peaks within the energy gap region of the CNT. The position of these peaks is quite independent of the nanotube length, but their heights decay exponentially with it. These peaks are associated with defect states localized at the interface between graphene and the nanotube. Gonzalez et al.,[8] predicted this kind of states confined at the interface between metallic nanotubes and graphene, under certain conditions. Here, we find them also for the case of semiconducting nanotubes. Figure 4a shows an example of such a state for the case of the #6 link for the (8,0) nanotube. The state plotted is responsible for the transmission peak just above the Fermi level for this link (see Figure 3d), and there is a similar one which accounts for the peak below the Fermi energy. The localized nature of these states explains the evolution of the transmission peaks with nanotube length (unchanged energy position but decreasing height).

The distinct behavior of the transmission curves for metallic and semiconducting nanotubes is more clearly evidenced in Figure 5, which shows the conductance
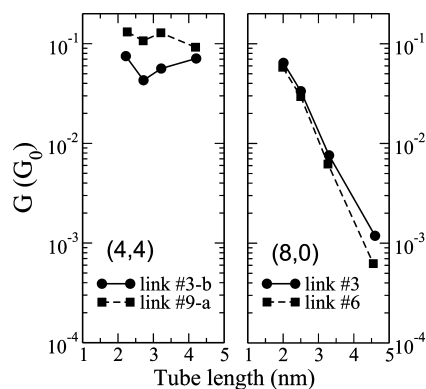
Figure 5. Conductance $G = I/V$ computed for a voltage of 0.6 V, for the (4,4) and (8,0) nanotubes (left and right panels, respectively), as a function of nanotube length. Symbols show values computed for different link structures, following Figure 1. Lines are just to guide the eye.

$G = I/V$ at a finite voltage of 0.6 V. This is obtained by integrating the transmission curves shown in Figure 3 (obtained in the limit of small voltages), in an energy window of 0.6 V centered at the Fermi energy. This represents an average of the transmission curves in the energy window considered, which washes out the details in the structure of peaks and reveals the main trends with respect to CNT length and link structure. Here we can see clearly that the conductance of the metallic (4,4) CNT is not very sensitive to the nanotube length, but changes significantly with the structure of the link. The average conductance is, nevertheless, significantly smaller than the maximum intrinsic conductance of the nanotube ($2G_0$). For the semiconducting tube the behavior is the opposite: the finite voltage conductance changes exponentially with the length of the tube (as corresponds to the tunneling regime), but is mainly independent of the structure of the link (despite the fact that the transmission curves are significantly different, as discussed above).

We now analyze the transmission curves presented in Figure 3 in terms of contributions from different eigenchannels of the transmission matrix and for different $k_\parallel$-points along the direction of the graphene edge. For illustration, in Figure 6 we show the results for a 4.2 nm long (4,4) nanotube, connected to graphene with #9-a links. In each panel, two transmission eigenchannels are shown for a particular $k_\parallel$-point (other eigenchannels give negligible contribution to the total transmission). We will first focus on the top panel, which corresponds to a $k_\parallel$-point which contains the K-point of the graphene Brillouin zone; for this point, graphene supports states at all energies in the window considered, since the Dirac point is contained in the sampling. For each of the two nonvanishing eigenchannels, the transmission is made up of resonances which correspond to transmitting states of the nanotube at particular energies. These resonances have maxima with large transmission values, often very close to 1, as corresponds to discrete contact states coupled symmetri-
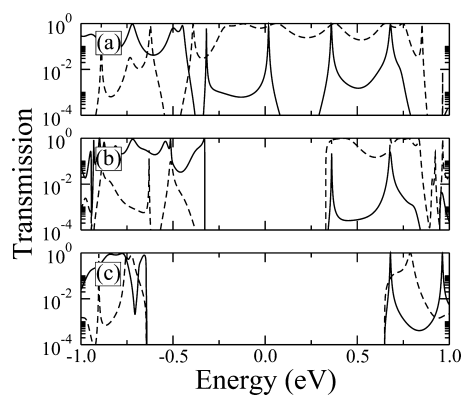

Figure 6. Transmission curves resolved in $k_\parallel$ (along the direction of the graphene edge) for the two main transmission eigenchannels for the 4.2 nm long (4,4) nanotube with #9-a links, for three different $k_\parallel$-points. In panel a, the $k_\parallel$-point contains the Dirac point of graphene. Panels b and c are for $k_\parallel$-points with increasing distance from it.

cally to wide-band electrodes. The effect of having a different link structure to each graphene sheet, leading to asymmetric contact structures, will likely yield resonances with lower transmission (work in this direction is underway).

To gain insight into the nature of the two transmission eigenchannels, we have calculated the corresponding scattering states[17,18] (using the Inelastica code[19]) for several energies. We find that the two transmission eigenchannels shown in Figure 6 with full and dashed lines correspond closely to standing waves of the finite nanotube originating from the CNT bonding (π) and antibonding (π^*) states,[20] respectively, which couple to states of graphene with the similar character. This is shown in Figure 4b,c which plots the scattering states computed at 0.36 eV (where both transmission eigenchannels show maxima in Figure 6a.). Plots at different energies show states with similar character, but different numbers of nodes along the carbon nanotube, as expected from the energy *versus* wavelength dependence of the standing waves. The width of the resonances, which reflects the efficiency of the coupling of the CNT waves with the graphene states, depends on both the specific eigenchannel and energy.

Careful inspection of Figure 6a shows an effect that was not easily identified in the total transmission curves of Figure 3: there is a clear offset between the band structure of the (4,4) nanotube and that of graphene. Ideally, in a zone-folding approach or a simple π orbital TB Hamiltonian description, the energies of the Dirac point (Fermi level) of graphene and that of the metallic nanotubes are the same, and there is no band offset between both systems. However, the transmission curves in Figure 6a clearly shows that the (4,4) CNT states are shifted by about 0.2 eV above the Fermi level of graphene. This offset is due to the finite and small radius of the nanotube, and its value is in close agreement with the difference in work functions of ideal, infinite (4,4) CNT and graphene, as calculated by Shan and

Cho.[21] For the (4,4) nanotube, the offset obtained is nearly the same for both CNT−graphene links, unlike in the case of the (8,0) nanotube discussed above, which depends strongly on the link structure and the associated strain. These band offset effects, which can be very relevant for electronic transport properties, are straightforwardly obtained from first-principles calculations as those presented here, whereas they are completely absent from simplified descriptions such as π orbital TB Hamiltonians.

We now turn to the discussion of the $k_\parallel$ dependence of the transmission curves, as shown in Figure 6. The transmission at the Fermi level is nonzero only for the $k_\parallel$-point which contains the K-point of the graphene Brillouin zone (top panel), since only there does graphene support electronic states at that energy. For other $k_\parallel$-points, the transmission shows a gap corresponding to the one in the bulk graphene band structure projected at that surface $k_\parallel$-point. Following the shape of the Dirac cones, the size of the gap increases linearly with the distance to the K-point. Upon $k_\parallel$ averaging, the transmission at the Fermi energy goes to zero, as can be seen in all the curves in Figure 3, following the V-shaped density of states of graphene (this can be seen more clearly in the inset in Figure 3b). This reflects the fact that, for infinite graphene, only two channels contribute at the Fermi level (the two states at the Dirac point), giving a total conductance of $2G_0$ for the whole graphene sheet, so that the conductance *per supercell* (which is what is calculated here) drops to zero. Therefore, the drop in the transmission and conductance at the Fermi level in our calculation is related to the finite number of channels of graphene, rather than to the scattering properties of the nanotube contacts. In this sense, graphene acts as a rather peculiar bulk electrode, since around the Fermi level it sustains fewer conduction channels than the contact (the periodic arrangement of nanotubes has two channels *per nanotube*), so the conductance of our system around the Fermi level is determined by the electrode rather than the contact. To extract conclusions about the conductance of a *single* nanotube contact between graphene sheets, we should replace the periodic image setup by a single nanotube contact. Alternatively, we can compute the conductance of a given supercell with a nanotube link, normalized by the conductance of the same graphene supercell, which yields the average transmission per incoming graphene channel. This actually removes the drop of the conductance at the Fermi level and leads to transmission curves with a resonance structure similar to the $k_\parallel$-resolved ones shown in Figure 6. We should finally note that, as shown by Gonzalez et al.,[8] suppression of the transmission probability for graphene states at small energies around the Fermi level is also possible in contacts of a single nanotube with infinite graphene due to symmetry mismatch between the wave functions of both systems. We have not observed this suppression in the nanotube arrays sandwiched between semi-infinite graphene sheets studied here, as shown in Figure 6a.

CONCLUSIONS

We have presented first-principles calculations of the structure and transport properties of links between metallic and semiconducting nanotubes between two graphene layers. We have shown the common features for both kinds of nanotubes (large, ballistic conductance for energies within the band regions), and the distinct behavior around the Fermi level. The semiconducting nanotube contacts are characterized by a conductance which decreases exponentially with nanotube length for energies within the band gap of the nanotube, and nearly independent of the structure of the link. Metallic tubes, on the other side, show a conductance that is quite independent of the nanotube length but sensitive to the structure of the link between CNT and graphene. Effects of band alignment have been found in the range of several tenths of eV, which can only be described by means of first-principles calculations. We have shown the character of the conducting states as resonances of nanotube standing waves and identified states which are localized at the graphene-nanotube link.

METHODS

Our first-principles calculations are based on density functional theory (DFT) as implemented in Siesta.[22−24] We use the GGA functional in the PBE form,[25] Troullier-Martins pseudopotentials,[26] and a basis set of finite-range numerical pseudoatomic orbitals for the valence wave functions.[27] For the equilibrium structures (relaxed using a double-ζ polarized basis[27]) we calculate the conductance from first-principles, using a single-ζ basis set, by means of the TranSiesta method,[14] within the nonequilibrium Green's function (NEGF) formalism. The graphene−CNT connections (including the H terminations at the graphene edge) were relaxed within the scattering region (green in Figure 2), using a slanted supercell geometry. The atoms in the leads (blue atoms in Figure 2) were forced to remain at the ideal planar graphene structure.

REFERENCES AND NOTES

1. Charlier, J.-C.; Blase, X.; Roche, S. Electronic and Transport Properties of Nanotubes. *Rev. Mod. Phys.* **2007**, *79*, 677.
2. Castro-Neto, A. H.; Guinea, F.; Peres, N. M. R.; Novoselov, K. S.; Geim, A. K. The Eletronic Properties of Graphene. *Rev. Mod. Phys.* **2009**, *81*, 109–162.
3. Ferry, D. K. Materials Science: Nanowires in Nanoelectronics. *Science* **2008**, *319*, 579–580.

4. Li, Y.-F.; Li, B.-R.; Zhang, H.-L. The Computational Design of Junctions between Carbon Nanotubes and Graphene Nanoribbons. *Nanotechnology* **2009**, *20*, 225202.

5. Kondo, D.; Sato, S.; Awano, Y. Self-Organization of Nobel Carbon Composite Structure: Graphene Multi-Layers Combined Perpendicularly with Aligned Carbon Nanotubes. *Appl. Phys,. Express* **2008**, *1*, 074003.

6. Kane, A. A.; Sheps, T.; Branigan, E. T.; Apkarian, V. A.; Cheng, M. H.; Hemminger, J. C.; Hunt, S. R.; Collins, P. G. Graphite Electrical Contacts to Metallic Single-Walled Carbon Nanotubes Using Pt Electrodes. *Nano Lett.* **2009**, *9*, 3586–3591.

7. Matsumoto, T.; Saito, S. Geometric and Electronic Structure of New Carbon-Network Materials: Nanotube Array on Graphite Sheet. *J. Phys. Soc. Jpn.* **2002**, *71*, 2765–2770.

8. González, J.; Guinea, F.; Herrero, J. Propagating, Evanescent and Localized States in Carbon Nanotube−Graphene Junctions. *Phys. Rev. B* **2009**, *79*, 165434.

9. Dimitrakakis, G. K.; Tylianakis, E.; Froudakis, G. E. Pillared Graphene: A New 3-D Network Nanostructure for Enhancing Hydrogen Storage. *Nano Lett.* **2008**, *8*, 3166–3170.

10. Varshney, V.; Patnaik, S. S.; Roy, A. K.; Froudakis, G.; Farmer, B. L. Modeling of Thermal Transport in Pillared-Graphene Architectures. *ACS Nano* **2010**, *4*, 1153–1161.

11. Saito, M.; Fujita, R.; Dresselhaus, G.; Dresselhaus, M. S. Electronic Structure of Chiral Graphene Tubules. *Appl. Phys. Lett.* **1992**, *60*, 2204–2206.

12. Wildoer, J. W. G.; Venema, L. C.; Rinzler, A. G.; Smalley, R. E.; Dekker, C. Electronic Structure of Atomically Resolved Carbon Nanotubes. *Nature* **1998**, *391*, 59–62.

13. Baowan, D.; Cox, B. J.; Hill, J. M. Two Least Squares Analyses of Bond Lengths and Bond Angles for the Joining of Carbon Nanotubes to Graphenes. *Carbon* **2007**, *45*, 2972–2980.

14. Brandbyge, M.; Mozos, J.-L.; Ordejón, P.; Taylor, J.; Stokbro, K. Density-Functional Method for Nonequilibrium Electron Transport. *Phys. Rev. B* **2002**, *65*, 165401.

15. Datta, S. *Electronic Transport in Mesoscopic Systems*; Cambridge University Press: Cambridge, UK, 2007.

16. Thygesen, K. S.; Jacobsen, K. W. Interference and k-Point Sampling in the Supercell Approach to Phase-Coherent Transport. *Phys. Rev. B* **2005**, *72*, 033401.

17. Frederiksen, T.; Paulsson, M.; Brandbyge, M.; Jauho, A.-P. Inelastic Transport Theory from First Principles: Methodology and Application to Nanoscale Devices. *Phys. Rev. B* **2007**, *75*, 205413.

18. Paulsson, M. Brandbyge, Transmission Eigenchannels from Nonequilibrium Green's Functions. *Phys. Rev. B* **2007**, *76*, 115117.

19. INELASTICA can be downloaded from http://sourceforge.net/projects/inelastica.

20. Rubio, A.; Sánchez-Portal, D.; Artacho, E.; Ordejón, P.; Soler, J. M. Electronic States in a Finite Carbon Nanotube: A One-Dimensional Quantum Box. *Phys. Rev. Lett.* **1999**, *82*, 3520–3523.

21. Shan, B.; Cho, K. First-Principles Study of Work Functions of Single Wall Carbon Nanotubes. *Phys. Rev. Lett.* **2005**, *94*, 236602.

22. Ordejón, P.; Artacho, E.; Soler, J. M. Self-Consistent Order-N Density-Functional Calculations for Very Large Systems. *Phys. Rev. B* **1996**, *53*, R10441–R10444.

23. Soler, J. M.; Artacho, E.; Gale, J. D.; García, A.; Junquera, J.; Ordejón, P.; Sánchez-Portal, D. The SIESTA Method for *ab Initio* Order-N Materials Simulation. *J. Phys.: Condens. Matter* **2002**, *14*, 2745–2779.

24. Artacho, E. The SIESTA Method: Developments and Applicability. *J. Phys.: Condens. Matter* **2008**, *20*, 064208.

25. Perdew, J. P.; Burke, K.; Ernzerhof, M. Generalized Gradient Approximation Made Simple. *Phys. Rev. Lett.* **1996**, *77*, 3865–3868.

26. Troullier, N.; Martins, J. L. Efficient Pseudopotentials for Plane-Wave Calculations. *Phys. Rev. B* **1991**, *43*, 1993–2006.

27. Artacho, E.; Sánchez-Portal, D.; Ordejón, P.; García, A.; M. Soler, J. Linear-Scaling *ab-Initio* Calculations for Large and Complex Systems. *Phys. Stat. Sol. (B)* **1999**, *215*, 809–817.